Supporting information

Multiphase Complex Coacervate Droplets

Tiemei Lu and Evan Spruijt*

Radboud University, Institute for Molecules and Materials, Heyendaalseweg 135, 6525 AJ Nijmegen, the Netherlands

Extended methods

Polymers

- Poly(diallyl dimethylammonium chloride) (**PDDA**, 200-350 kDa, 20 wt% solution in H_2O) was purchased from Sigma and diluted with Milli-Q water to at a stock concentration of 50 mg/mL (0.31 M in monomer units).
- Poly(allylamine hydrochloride) (**PAH**, 58 kDa) was purchased from Sigma and dissolved in Milli-Q water at a stock concentration of 10 mg/mL (0.11 M in monomer units). Tetramethylrhodamine labeled PAH (PAH-TAMRA) was prepared by carbodiimide mediated coupling reaction with EDC and NHS following a previous report.[1] The molar ratio of TAMRA:EDC:NHS = 1:1.5:1.5 and the volume of DMSO was 10% of the total reaction volume.
- Dextran sulfate sodium salt (**S-Dex**, from Leuconostoc spp., 9-20 kDa) was purchased from Sigma and dissolved in Milli-Q water at a concentration of 100 mg/mL.
- Poly(acrylic acid) (**PAA**, 15 kDa, 35 wt% solution in H_2O) was diluted by Milli-Q water to a concentration of 61 mg/mL.
- Adenosine 5′-triphosphate disodium salt hydrate (**ATP**) was freshly dissolved in Milli-Q water at a concentration of 100 mM and kept on ice throughout the experiments.
- Poly-L-lysine hydrobromide (**PLys**, 52 kDa) was purchased from Alamanda polymers and was dissolved in Milli-Q water at a concentration of 50 mg/mL (0.24 M in monomer units). Tetramethylrhodamine labeled PLys (PLys-TAMRA) was prepared in the same way as PAH-TAMRA.
- Trimethylated poly-L-lysine (**PLys(Me)$_3$**) was prepared from PLys, according to a previously published article and was dissolved in Milli-Q water at a concentration of 100 mM.[2]
- Single-stranded DNA (**ssDNA**, 43 nt) was purchased from Biomers (sequence: GCCTCGAATCACTCCACTGAACCATCCTCTTGATCTTGTGAAC) and was dissolved in Milli-Q water at a concentration of 2.0 mg/mL. Alexa-647 labeled ssDNA was prepared according to a previously reported procedure.[3]
- Poly (2-(methacryloyloxy)ethyltrimethylammonium chloride) (**PMETAC**, 25 kDa, PDI 1.26) was prepared by living atom transfer radical polymerization as reported previously,[4] and dissolved in Milli-Q water at a concentration of 50 mg/mL (0.24 M in monomer units).
- Poly(3-sulfopropyl methacrylate) (**PSPMA**, 30 kDa, PDI 1.3) and PSPMA copolymer with 10 mol% fluorescein methacrylate (**PSPMA-Fl**, 48 kDa, PDI 1.13) were prepared by living atom transfer radical polymerization as reported previously.[4] The polymers were dissolved in Milli-Q water at a concentration of 50 mg/mL (0.24 M in monomer units) and 10 mg/mL, respectively.
- Poly-D-glutamate (**PGlu**, 5.6 kDa, PDI 1.06) was prepared by free radical polymerization of O-benzyl-D-Glutamate-*N*-carboxyanhydride, followed by deprotection, as described elsewhere,[5] and was dissolved in Milli-Q water at a concentration of 13 mg/mL (0.1 M in monomer units).
- Glycidyl trimethylammonium chloride functionalized dextran (**Q-Dex**, 150 kDa) was prepared following a previous report,[6] and was dissolved in Milli-Q water at a concentration of 50 mg/mL.
- Diethylaminoethyl-functionalized dextran (**DEAE-Dex**, 150 kDa) was prepared following a previous report,[7-8] and was dissolved in Milli-Q water at a concentration of 50 mg/mL.
- GFP-K_{72} (80 μM) was obtained by expression in *E.coli* and purification by affinity and size exclusion chromatograph as described previously.[9]

Supplementary tables

Table S1. Molecular structures of polycations and polyanions.

Negatively charged polymers	Structure	Positively charged polymers	Structure
PSPMA	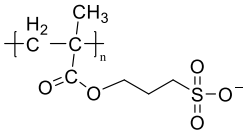	PDDA	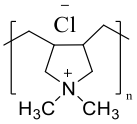
S-Dex	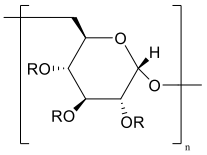 R = H or SO_3Na	$PLys(Me)_3$	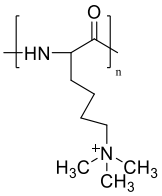
ATP	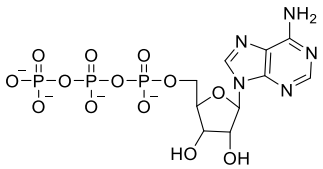	PMETAC	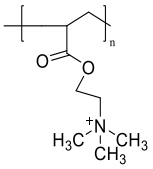
ssDNA	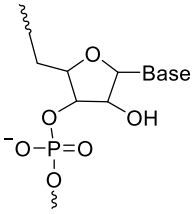	Q-Dex	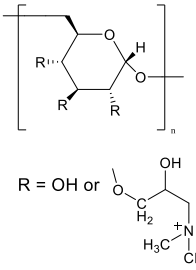
PAA	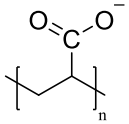	DEAE-Dex	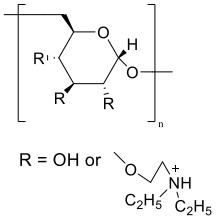
PGlu	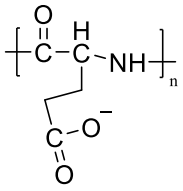	PAH	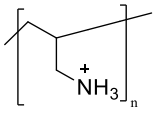
		PLys	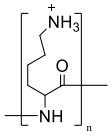
		GFP-K_{72}	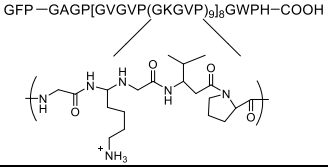

Table S2. Single complex coacervates.

Coacervates formation			(poly) cation							
				-NR_3^+			-NHR_2^+		-NH_3^+	
			PDDA	PLys(Me)$_3$	PMETAC	Q-Dex	DEAE-Dex	PAH	GFP-K_{72}	PLys
(poly) anion	-$SO_{3/4}^-$	PSPMA	√	√	√	√	√	√	√	√
		S-Dex	√	√	√	√	/	↓	√	↓
	-PO_4^-	ATP	√	√	√	solution	/	√	√	√
		ssDNA	√	√	√	√	/	√	√	√
	-CO_2^-	PAA	√	√	√	√	/	√	√	↓
		PGlu	√	√	√	√	/	√	solution	√

Table S3. Salt concentrations at which coacervates were prepared.

Coacervates formation NaCl concentration (M)			(poly) cation							
				-NR_3^+			-NHR_2^+		-NH_3^+	
			PDDA	PLys(Me)$_3$	PMETAC	Q-Dex	DEAE-Dex	PAH	GFP-K_{72}	PLys
(poly) anion	-$SO_{3/4}^-$	PSPMA	0.50	0.50	0.50	0.20	0.40	1.0	0.20	0.50
		S-Dex	1.0	0.50	0.50	0.40	/	↓	0.30	↓
	-PO_4^-	ATP	0.050	0.0060	0.020	solution	/	1.0	0.010	0.040
		ssDNA	0.050	0.040	0.050	0.040	/	0.050	0.050	0.050
	-CO_2^-	PAA	0.30	0.27	0.30	0.15	/	1.0	0.15	↓
		PGlu	0.20	0.30	0.30	0.15	/	0.60	solution	0.40

Table S4. Multiphase complex coacervate droplets prepared from combinations in Table S2.

No.	Coacervate 1	Coacervate 2	Coacervate 3	Multiphase	Components
1	ssDNA/PLys(Me)$_3$	ssDNA/GFP-K_{72}	/	Two	3
2	ATP/PDDA	ATP/PAH	/	Two	3
3	PAA/PLys(Me)$_3$	PAA/GFP-K_{72}	/	Two	3
4	PGlu/PDDA	PGlu/PAH	/	Two	3
5	S-Dex/PLys(Me)$_3$	S-Dex/GFP-K_{72}	/	Two	3
6	PSPMA/PDDA	PSPMA/PAH	/	Two	3
7	PSPMA/DEAE-Dex	PSPMA/PAH	/	Two	3
8	PSPMA/PDDA	PSPMA/Q-Dex	/	Two	3
9	PSPMA/PDDA	ATP/PAH	/	Two	4
10	PSPMA/PLys(Me)$_3$	PSPMA/PAH	/	Two	3
11	PSPMA/PMETAC	PSPMA/PAH	/	Two	3
12	PSPMA/PLys(Me)$_3$	PSPMA/GFP-K_{72}	/	Two	3

13	PSPMA/PAH	PSPMA/PLys	/	Two	3
14	PSPMA/Q-Dex	PSPMA/PAH	/	Two	3
15	PGlu/PLys(Me)$_3$	PGlu/PLys	/	Two	3
16	PSPMA/PMETAC	PSPMA/PLys	/	Two	3
17	PGlu/Q-Dex	PGlu/PLys	/	Two	3
18	PSPMA/PDDA	PAA/PDDA	/	Two	3
19	PSPMA/PLys(Me)$_3$	PAA/PLys(Me)$_3$	/	Two	3
20	PSPMA/PDDA	PGlu/PDDA	/	Two	3
21	PSPMA/PDDA	ATP/PAH	PAA/PDDA	Three	5
22	PSPMA/PDDA	PSPMA/PAH	PSPMA/Q-Dex	Three	4
23	PSPMA/PDDA	PSPMA/PAH	PSPMA/DEAE-Dex	Three	4

Table S5. Critical salt concentrations of single complex coacervates.

Critical NaCl concentration (M)			**(poly) cation**							
				-NR_3^+			**-NHR_2^+**		**-NH_3^+**	
			PDDA	PLys(Me)$_3$	PMETAC	Q-Dex	DEAE-Dex	PAH	GFP-K_{72}	PLys
(poly) anion	**-$SO_{3/4}^-$**	PSPMA	1.0	0.82	1.0	0.36	0.69	2.6	0.30	1.2
		S-Dex	1.6	1.0	1.7	0.42	/	> 2.0	0.39	> 2.0
	-PO_4^-	ATP	0.088	0.010	0.030	< 0.020	/	2.4	0.050	0.17
		ssDNA	0.34	0.21	0.36	< 0.020	/	1.6	0.11	0.42
	-CO_2^-	PAA	0.39	0.36	0.48	0.20	/	> 3.6	0.27	/
		PGlu	0.36	0.32	0.38	0.14	/	2.8	/	0.87

Supplementary figures

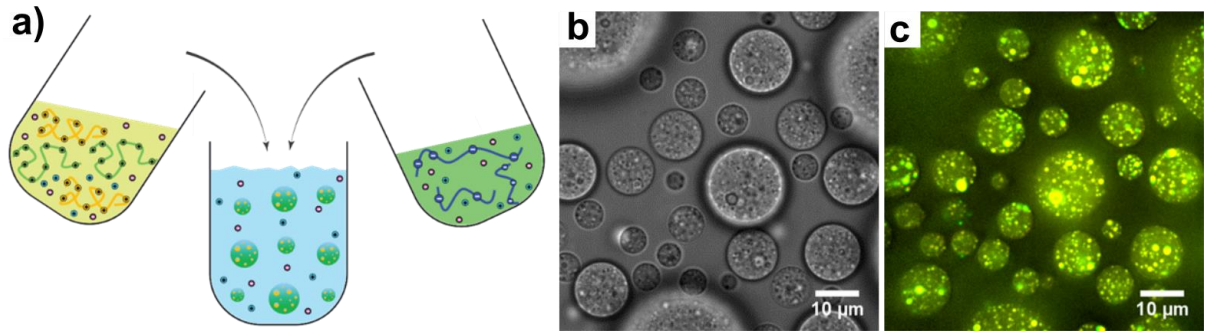

Figure S1. (a) Method 1 for preparing multiphase droplets by pre-mixing like-charged components, followed by combining them. (b,c) Bright-field and fluorescence images of PSPMA/PAH/PDDA multiphase droplets prepared with this method.

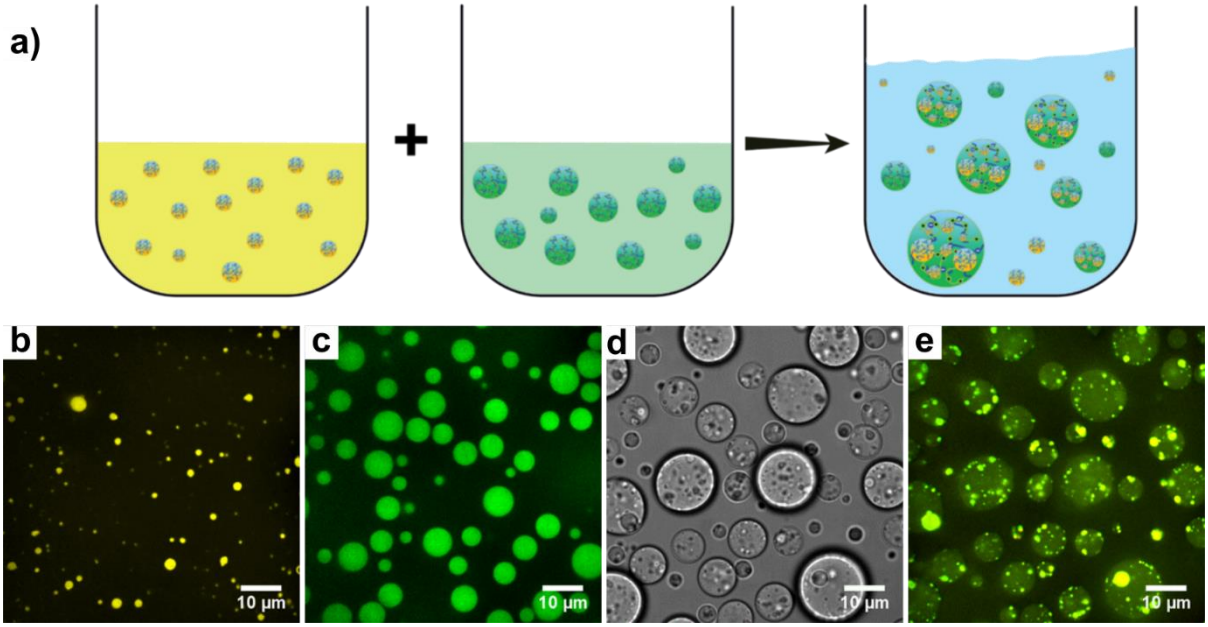

Figure S2. (a) Method 2 for preparing multiphase droplets by preparing single coacervates separately, followed by combining them. (b,c) Fluorescence images of the single coacervates of PSPMA/PAH and PSPMA/PDDA, respectively. (d,e) Bright-field and fluorescence images of the multiphase droplets prepared with this method.

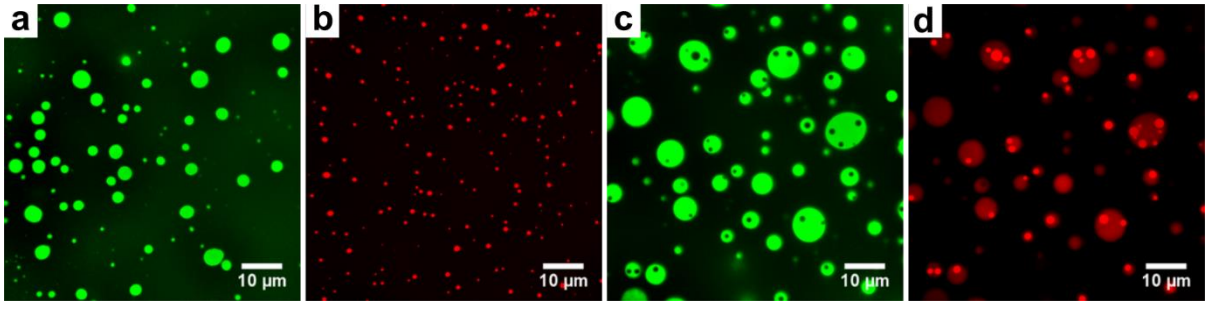

Figure S3. Single complex coacervates of (a) ssDNA/GFP-K_{72} and (b) ssDNA/PLys(Me)$_3$, and multiphase droplets shown in Figure 1b, obtained after combining (a) and (b), showing the separate channels for GFP-K_{72} (c) and ssDNA (d).

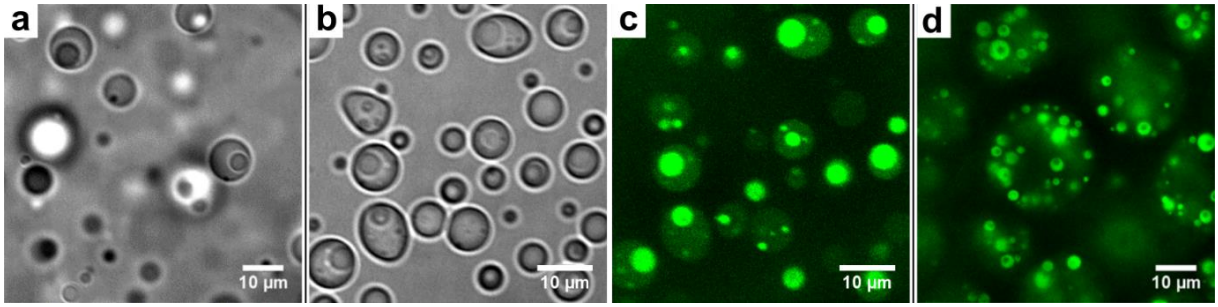

Figure S4. Multiphase coacervate droplets formed with two polyanions and a common polycation. (a) PSPMA/PLys(Me)$_3$ core coacervates in PAA/PLys(Me)$_3$ outer coacervate phases. (b,c) PSPMA/PDDA core coacervates in PGlu/PDDA outer phase coacervates visualized by bright-field (b) and fluorescence (c, PSPMA-Fl) microscopy. (d) PSPMA/PDDA core coacervates in PAA/PDDA outer phase coacervates visualized by fluorescence microscopy (PSPMA-Fl).

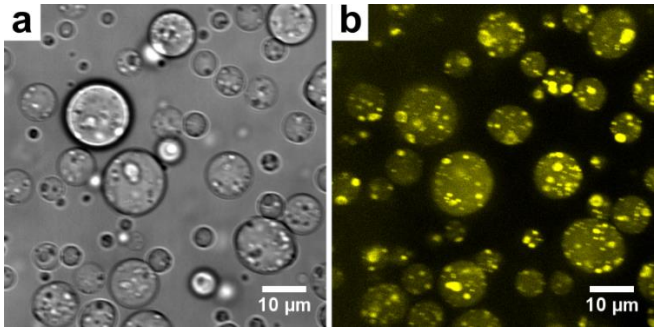

Figure S5. Multiphase coacervate droplets formed with a common polyanion and two primary amine polycations: PSPMA/PAH core coacervates in PSPMA/PLys outer phase coacervates, visualized by bright-field (a) and fluorescence (b, PAH-TAMRA) microscopy.

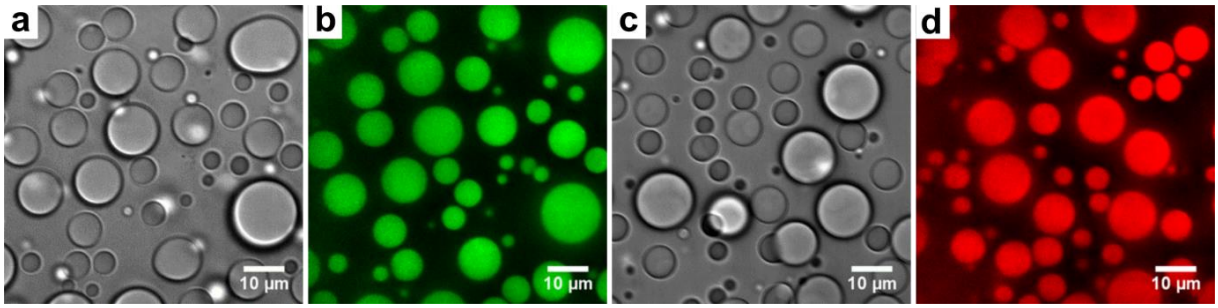

Figure S6. Single phase, mixed coacervate droplets formed after mixing two single phase coacervates with similar critical salt concentration. (a,b) PSPMA/PDDA and PSPMA/PMETAC, visualized by bright-field (a) and fluorescence (b, PSPMA-Fl) microscopy. (c,d) S-Dex/PDDA and S-Dex/PMETAC, visualized by bright-field (c) and fluorescence (d, ThT) microscopy.

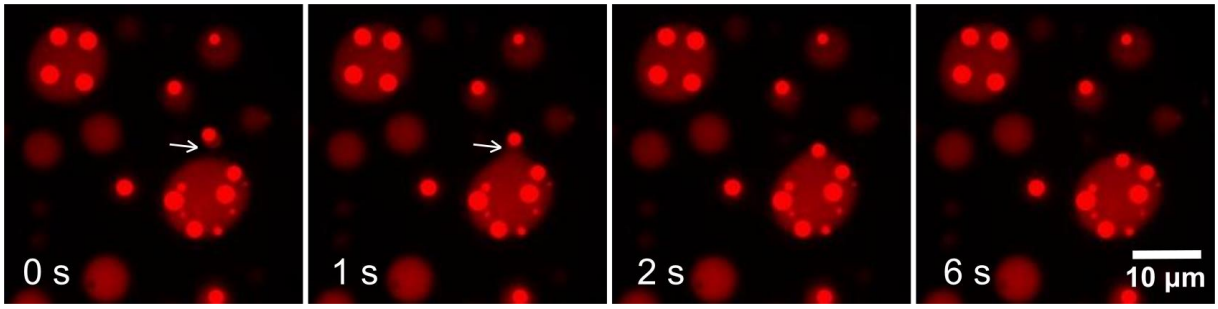

Figure S7. Engulfing of a ssDNA/PLys(Me)$_3$ coacervate by a ssDNA/GFP-K$_{72}$ coacervate (cf. Fig. 1b).

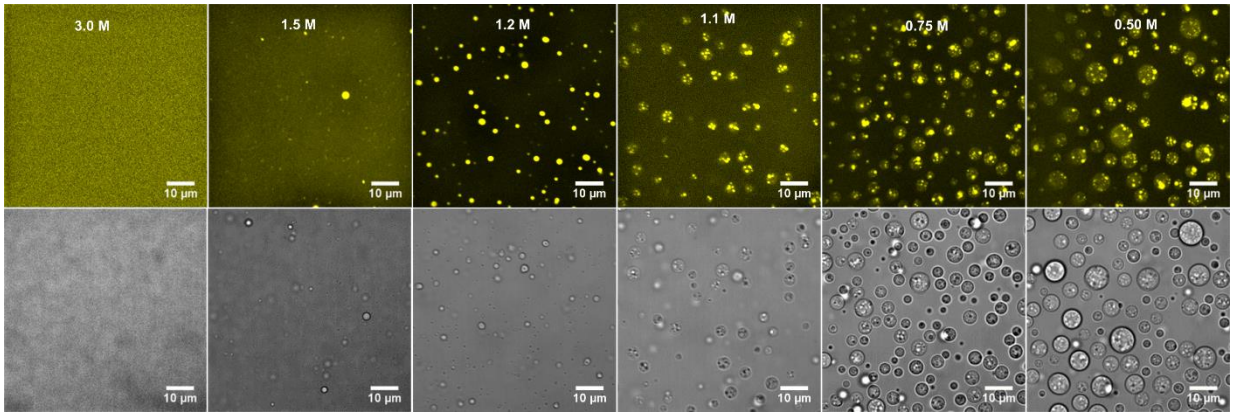

Figure S8. Step-wise condensation of PSPMA/PAH/PDDA multiphase droplets, shown by confocal fluorescence microscopy (top row) and bright-field (bottom row).

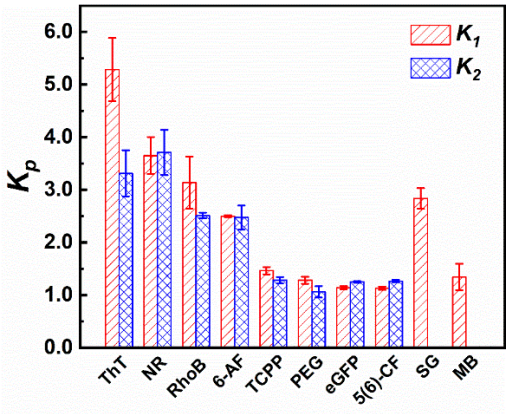

Figure S9. Partitioning coefficients of guest molecules shown in Figure 5 in the outer coacervate phase (K_1) and between the core coacervate and outer coacervate phase (K_2).

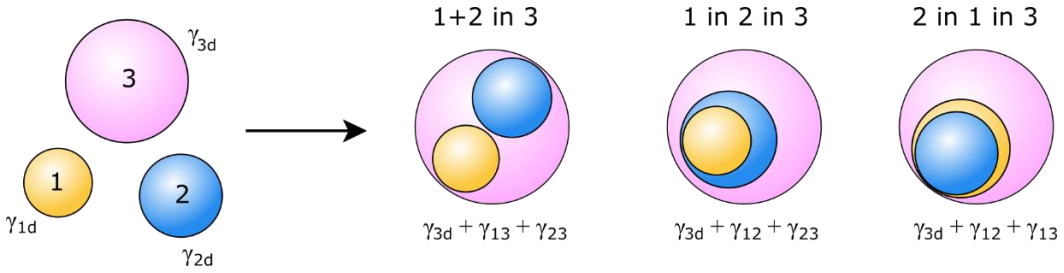

Figure S10. Schematic illustration of some of the possible arrangements of three immiscible coacervate phases. Coacervate 3 is assumed to have the lowest density and interfacial tension.

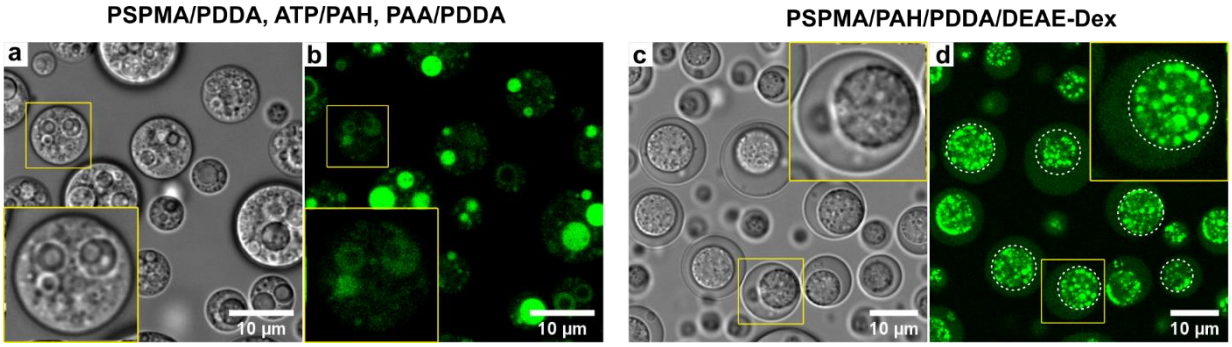

Figure S11. (a,b) An ATP/PAH inner core, surrounded by a PSPMA/PDDA shell in a PAA/PDDA outer coacervate phase (prepared by method 1). (c,d) PSPMA/PAH inner core, surrounded by a PSPMA/PDDA shell in a PSPMA/DEAE-Dex coacervate phase (prepared by method 1). All these samples are visualized at the same position in bright-field (a,c) and by confocal fluorescence microscopy (b,d) (PSPMA-Fl fluorescence). Because the core coacervates were not prepared at a high salt concentration before mixing with the other coacervates and lowering the salt concentration in this method, the cores appear more gel-like and irregular in shape than with method 2.

Mean-field theory of complex coacervates

The mean-field free energy density of a mixture of two components is given by:

$$\frac{F}{kT} = \frac{\phi}{N_1}\ln\phi + \frac{1-\phi}{N_2}\ln(1-\phi) + \chi\phi(1-\phi) \qquad \text{(S1)}$$

where the Flory interaction parameter χ is a measure for the interaction strength between the two components, relative to their self-interaction. Beyond a critical value of χ, phase separation occurs, and the binodal concentrations can be found from a common tangent construction, close to the spinodal points ($\partial^2 F/\partial\phi^2 = 0$).

In a symmetric mixture of polymers (N_1=N_2=N) in a single solvent, the tangent is horizontal, and the binodal concentrations are given by the implicit relation, under the assumption that both phases are equally hydrated:[10]

$$\chi_b N = -\frac{\ln(\phi) - \ln(1-\phi_w-\phi)}{(1-\phi_w-2\phi)} \qquad \text{(S2)}$$

Figure S12 shows the binodal concentrations calculated by Eq. S2 for two coexisting polymer solutions with a common solvent (e.g., aqueous two-phase system, or two coacervates). The segregation between the two phases increases with increasing χ (stronger interactions) up to a volume fraction of $(1-\phi_w)$ of each polymer in their respective phases.

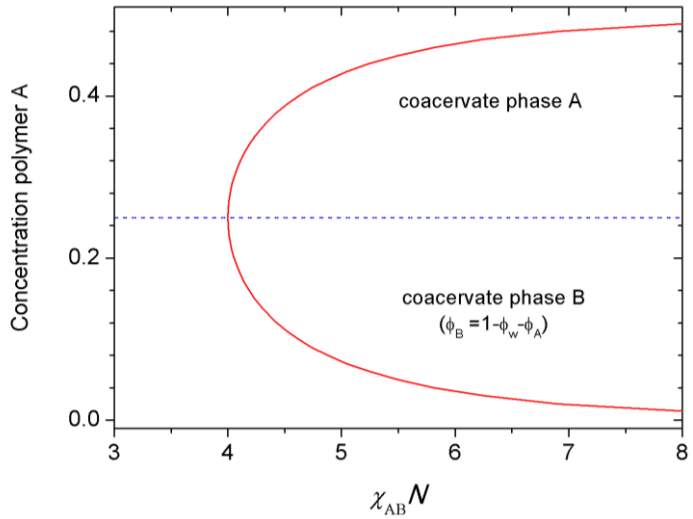

Figure S12. The binodal concentrations of two coexisting coacervates change with interaction parameter χ, for an equal degree of hydration of ϕ_w= 0.5.

The interfacial tension also increases with increasing χ away from the critical point as:[4]

$$\gamma \propto (\chi - \chi_c)^{3/2} \tag{S3}$$

For complex coacervation, the Flory-Huggins framework has been extended by Voorn and Overbeek with a Debye-Hückel approximation for the electrostatic interaction between oppositely charged species.[11-12] For complex coacervates composed of polymers of equal length (N) at a 1:1 charge ratio, the phase behaviour can be mapped onto the Flory-Huggins theory for a polymer in solution, by defining an effective interaction parameter:[12]

$$\chi_{\text{eff}} = \chi_r + \frac{\sqrt{\pi}}{3\sqrt{2N_{Av}}} \frac{\sigma^2}{\sqrt{c_s}} \left(\frac{\sqrt{l_B}}{l}\right)^3 \tag{S4}$$

where l is the lattice size, l_B the Bjerrum length, σ the charge density, c_s the ionic strength (in mM), and χ_r the residual, non-electrostatic part of the interaction parameter. The critical salt concentration c_s^* can be found by combining equation (S4) above and the expression for the critical χ_c of a polymer in solution: $\chi_c = \frac{1}{2} + \frac{1}{\sqrt{N}}$, resulting in:[12]

$$c_s^* = \frac{\pi}{18N_{Av}} \left(\frac{l_B}{l^2}\right)^3 \frac{\sigma^4}{\left(\frac{1}{2} + \frac{1}{\sqrt{N}} - \chi_r\right)^2} \tag{S5}$$

$$\chi_{\text{eff}} = \frac{1}{2} + \frac{1}{\sqrt{N}} + \frac{\sqrt{\pi}\,\sigma^2}{3\sqrt{2N_{Av}}} \left(\frac{\sqrt{l_B}}{l}\right)^3 \left(\frac{1}{\sqrt{c_s}} - \frac{1}{\sqrt{c_s^*}}\right) \tag{S6}$$

According to these equations, the higher the critical salt concentration of a complex coacervate, the larger its effective interaction parameter, and the larger its density and interfacial tension at a given salt concentration (as shown in Figure S13).

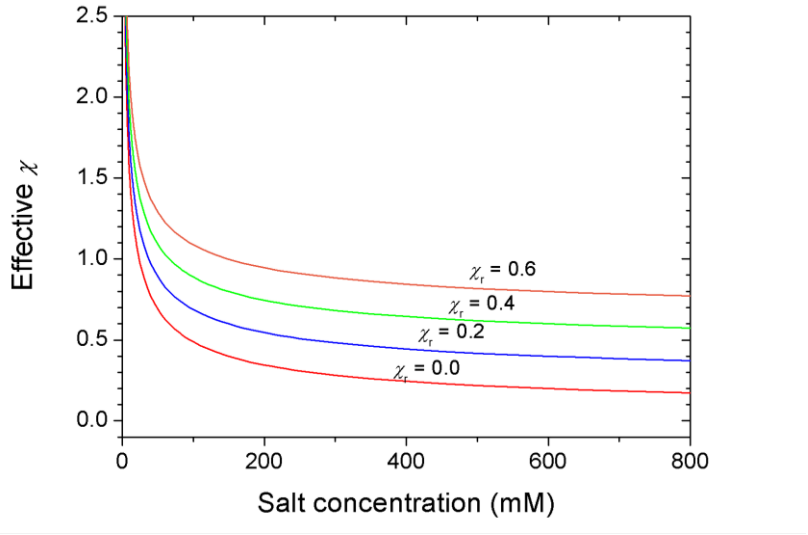

Figure S13. The relationship of effective interaction parameter χ with salt concentration.

Finally, the effective interaction between two coexisting coacervates, χ_{12}, can be approximated using an expression for the polymer-polymer interaction in phase separated solutions (see main text), which ultimately results in:

$$\chi_{12} \approx \frac{\pi\sigma^4}{36N_{\mathrm{Av}}}\left(\frac{l_B}{l^2}\right)^3\left(\frac{1}{\sqrt{c_1^*}}-\frac{1}{\sqrt{c_2^*}}\right)^2 \approx 0.1\left(\frac{1}{\sqrt{C_1^*}}-\frac{1}{\sqrt{C_2^*}}\right)^2 \quad \text{(S7)}$$

where the second approximation is valid for strongly charged polyelectrolytes ($\sigma \approx 1$), and the parameters used in Ref. 12. C_1^* and C_2^* are the two critical salt concentrations in mol/L.

Supplementary movies

Movie S1. Fusion of core PAA/PLys(Me)$_3$ coacervates inside a PAA/GFP-K$_{72}$ outer phase (Figure 2a), 6x real time.

Movie S2. Fusion of PGlu/PDDA coacervates followed by fusion of their internal PGlu/PAH cores (Figure 2b), 2.5x real time.

Movie S3. Fusion of PSPMA/PDDA coacervates inside a PSPMA/Q-Dex coacervate, 2.5x real time.

Movie S4. Engulfing of an ATP/PAH coacervate by a PSPMA/PDDA coacervate (Figure 2c), 2x real time.

Movie S5. Fusion of intermediate PSPMA/PDDA coacervates inside a PAA/PDDA coacervate, followed by fusion of the inner ATP/PAH core coacervates (Figure 6a-b), 2.5x real time.

Supplementary references

1. Wang, F.; Zhang, D.; Duan, C.; Jia, L.; Feng, F.; Liu, Y.; Wang, Y.; Hao, L.; Zhang, Q., Preparation and characterizations of a novel deoxycholic acid–O-carboxymethylated chitosan–folic acid conjugates and self-aggregates. *Carbohydrate polymers* **2011,** *84* (3), 1192-1200.

2. Granados, E. N.; Bello, J., Alkylated poly(amino acids). I. Conformational properties of poly(N^{ϵ}-trimethyl-L-lysine) and poly(N^{δ}-trimethyl-L-ornithine). *Biopolymers* **1979,** *18*, 1479-1486.

3. Spruijt, E.; Tusk, S. E.; Bayley, H., DNA scaffolds support stable and uniform peptide nanopores. *Nature nanotechnology* **2018,** *13* (8), 739-745.

4. Spruijt, E.; Sprakel, J.; Cohen Stuart, M. A.; van der Gucht, J., Interfacial tension between a complex coacervate phase and its coexisting aqueous phase. *Soft Matter* **2010,** *6* (1), 172-178.

5. Cheng, J.; Deming, T. J., Synthesis of polypeptides by ring-opening polymerization of alpha-amino acid N-carboxyanhydrides. *Top Curr Chem* **2012,** *310*, 1-26.

6. Kalaska, B.; Kaminski, K.; Sokolowska, E.; Czaplicki, D.; Kujdowicz, M.; Stalinska, K.; Bereta, J.; Szczubialka, K.; Pawlak, D.; Nowakowska, M.; Mogielnicki, A., Nonclinical evaluation of novel cationically modified polysaccharide antidotes for unfractionated heparin. *PLoS One* **2015,** *10* (3), e0119486.

7. Siewert, C.; Haas, H.; Nawroth, T.; Ziller, A.; Nogueira, S. S.; Schroer, M. A.; Blanchet, C. E.; Svergun, D. I.; Radulescu, A.; Bates, F.; Huesemann, Y.; Radsak, M. P.; Sahin, U.; Langguth, P., Investigation of charge ratio variation in mRNA - DEAE-dextran polyplex delivery systems. *Biomaterials* **2019,** *192*, 612-620.

8. Usher, T. C.; Patel, N., Manufacture of diethylaminoethyl dextrans. **1985**.

9. Te Brinke, E.; Groen, J.; Herrmann, A.; Heus, H. A.; Rivas, G.; Spruijt, E.; Huck, W. T. S., Dissipative adaptation in driven self-assembly leading to self-dividing fibrils. *Nature Nanotechnology* **2018,** *13* (9), 849-855.

10. Rubinstein, M.; Colby, R. H. *Polymer physics*; Oxford University Press: New York, **2003**, pp 140-154.

11. Overbeek, J. T. G.; Voorn, M. J., Phase separation in polyelectrolyte solutions. Theory of complex coacervation. *Journal of Cellular and Comparative Physiology* **1957,** *49*, 7-26.

12. Spruijt, E.; Westphal, A. H.; Borst, J. W.; Cohen Stuart, M. A.; van der Gucht, J., Binodal Compositions of Polyelectrolyte Complexes. *Macromolecules* **2010,** *43* (15), 6476-6484.